

Supporting information

Pushing the limits on the intestinal crossing of Metal-Organic Frameworks: an *ex vivo* and *in vivo* detailed study

Sara Rojas, Tania Hidalgo, Zhongrui Luo, David Ávila, Anna Laromaine,* Patricia Horcajada*

S1. Experimental techniques

^1H NMR experiments for the characterization of the synthesized ligand were recorded on an Advance Bruker Instrument (300 MHz). Fourier transformed infrared spectroscopy (FTIR) analyses were carried out on a Thermo Nicolet 6700 spectrometer (Thermo, USA). Thermogravimetric analyses (TGA) were performed using a Perkin Elmer STA 6000 with an air flow of $100\text{ mL}\cdot\text{min}^{-1}$ and a ramp of $5\text{ }^\circ\text{C}\cdot\text{min}^{-1}$. Elemental analyses (EA) were determined using a FLASH 2000 (ThermoScientific, USA). N_2 isotherms were obtained at 77 K using a Belsorp Max (Bel. Japan). Prior to the analysis, approximately 40 - 60 mg of material was evacuated following a two-step process: under vacuum at $200\text{ }^\circ\text{C}$ for 12 h (MIL-127) and $150\text{ }^\circ\text{C}$ for 3 h (CS@MIL-127) (Belprep, Bel Japan) and then, at $120\text{ }^\circ\text{C}$ for 5 h under secondary vacuum directly in the Belsorp Max instrument. Routine X-ray powder diffraction (XRPD) patterns were collected using a conventional PANalytical Empyrean powder diffractometer (PANalytical Lelyweg, Netherlands, θ - 2θ) using $\lambda\text{Cu K}_{\alpha 1}$, and $\text{K}_{\alpha 2}$ radiation ($\lambda = 1.54051$ and 1.54433 \AA). The XRD patterns were carried out with a 2θ scan between 5 - 20° with a step size of 0.013° and a scanning speed of $0.1^\circ\cdot\text{s}^{-1}$. Inductively coupled plasma atomic emission spectroscopy (ICP-OES) analyses were performed in a Perkin Elmer Optima 7300 DV. For particle size and ζ -potential determinations *ca.* 1 mg of material was dispersed in 10 mL of each media (MilliQ, Ringer, *lis*-SIF, *lis*-SIF-muc, *lis*-SIF-panc, DMEM and Ringer medium), being analyzed with a Malvern Nano-ZS, Zetasizer Nano series. Once the suspensions were prepared, a sonication step was followed (20% amplitude, 30 s), monitoring the particle size evolution during 24 h. Field Emission Gun Scanning Electron Microscopy (FEG-SEM) was carried out using a JEOL JSM 6335F microscope at 15 kV coupled with an Oxford Instruments X-Max 80 mm^2 unit. Transmission electron microscopy (TEM) images were taken with a JEM 1400 (Jeol, Tokyo, Japan) with a 120 kV acceleration voltage (point resolution 0.38 nm). For TEM studies, *ca.* 1 mg of sample was dispersed in 10 mL of absolute EtOH and sonicated with an ultrasound tip (UP400S, Hilscher, Teltow, Germany) at 20% amplitude for 10 s. For observation, 10 μL of the prepared solution was dropped over a copper TEM grid coated with holey carbon support film (Lacey Carbon, 300 mesh, copper, approx. grid hole size: 63 μm , TED PELLA Redding, CA, USA). To perform the histological observation, worms & rats tissues were first stained using Perls' Prussian blue dye for Fe-MOF identification and hematoxylin and eosin (only in rats tissues) for histological examination then, fixed overnight using an *i*) agarose (2 g of agarose in 100 mL of PBS (pH = 7.4)), and *ii*) *p*-formaldehyde (4% PFA) solution, respectively.

Quantification of H₄TazBz linker by high performance liquid chromatography (HPLC). The MIL-127 leached ligand was determined using a reversed phase HPLC system, a Jasco LC-4000 series system, equipped with a PDA detector MD-4015 and a multisampler AS-4150 controlled by ChromNav software (Jasco Inc). A Purple ODS reverse-phase column (5 μm, 4.6 x 150 mm, Análisis Vínicos) was employed. The mobile phase consisted of a 50:50 solutions (v/v) of buffer (0.04 M, pH = 2.5) and methanol (MeOH). The injection volume was set to 30 μL with a flow rate of 1 mL·min⁻¹ and a fixed column temperature of 25 °C. The standard calibration curve showed a good correlation ≥ 0.99 . The chromatogram of standard solution showed a retention time of 21.8 min (λ_{max} at 311 nm, **Figure S1**).

Preparation of the mobile phase PBS (0.04 M, pH = 2.5). NaH₂PO₄ (2.4 g, 0.02 mol) and Na₂HPO₄ (2.84 g, 0.02 mol) were dissolved in 1 L of Milli-Q water. The pH was then adjusted to 2.5 with H₃PO₄ ($\geq 85\%$).

Preparation of high buffered solution: PBS (0.5 M, pH = 2.5). NaH₂PO₄ (30 g, 0.25 mol) and Na₂HPO₄ (35.5 g, 0.25 mol) were dissolved in 1 L of Milli-Q water. The pH was then adjusted to 2.5 with H₃PO₄ ($\geq 85\%$).

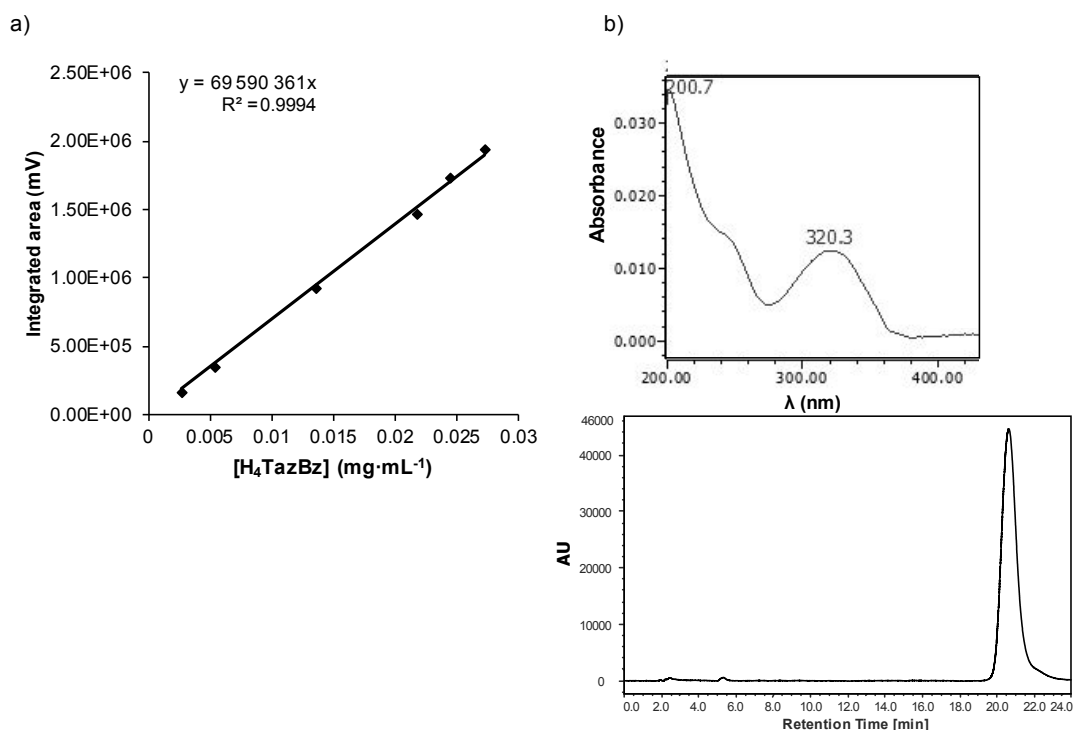


Figure S1. (a) Calibration plot of H₄TazBz by HPLC method, and (b) UV-vis spectrum and chromatogram of H₄TazBz.

S2. MIL-127 and CS@MIL-127 characterization

The amount of CS associated to the MIL-127 NPs was determined by combining ICP-OES, TGA and EA of different batches. After only 30 min contact time, the functionalized CS (expressed as percentage with respect to the dry NPs weight) reached ~35.5 %wt as deduced from the ICP-OES analysis, which is in rough agreement with the AE and TGA values (40.7 and 34.9%, respectively). Average: 37.0%.

MIL-127

$[\text{Fe}_3\text{O}(\text{OH})_{0.88}\text{Cl}_{0.12}(\text{C}_{16}\text{N}_2\text{O}_8\text{H}_6)_{1.5}](\text{H}_2\text{O})_5(\text{C}_2\text{H}_6\text{O})_{1.3}$. MW: 884.06 g·mol⁻¹.

ICP-OES Fe content. Calculated 18.9 %wt, found 14.7 ± 0.7 %wt.

Elemental analysis. Calculated N(4.75), C(35.82), H(3.15); found: N(4.73), C(36.04), H(2.73).

TGA residue after thermal treatment. Calculated: 27.1%; found: 25.7%.

CS@MIL-127

$[\text{Fe}_3\text{O}(\text{OH})_{0.88}\text{Cl}_{0.12}(\text{C}_{16}\text{N}_2\text{O}_8\text{H}_6)_{1.5}](\text{H}_2\text{O})_2(\text{C}_6\text{O}_5\text{H}_{11}\text{NH}_{0.2}(\text{COCH}_3)_{0.8})_{2,1}$. MW: 1193.71 g·mol⁻¹.

ICP-OES Fe content. Calculated 14.0 %wt, found 14.1 ± 0.7 %wt.

Elemental analysis. Calculated N(5.87), C(39.42), H(3.47); found N(6.25), C(39.44), H(3.75).

TGA residue after thermal treatment. Calculated: 19.7%; found: 19.5%.

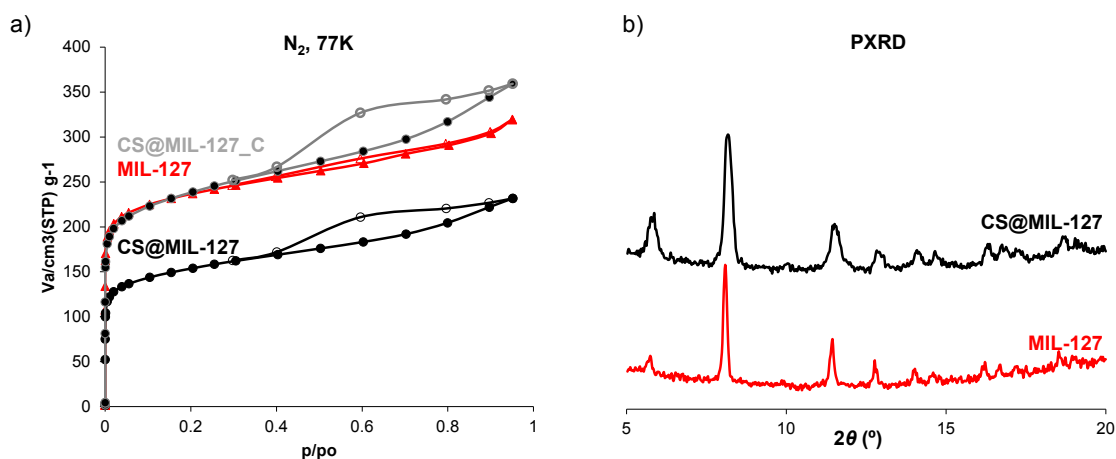


Figure S2. (a) N₂ sorption isotherms at 77 K and XRPD patterns of MIL-127 NPs before (red) and after CS-coating (black) after outgassing at 200 °C overnight and 150 °C for 3 h, respectively. Weight correction was also applied to obtain the corrected isotherm CS@MIL-127_C (grey), obtaining similar values than the original MIL-127 which confirm the presence of CS only on the external surface of the MOF NPs. Empty symbols denote desorption. (b) Although a peak broadening is observed in comparison with the bulk material, consistent with the smaller particle size, the full width at half maximum (FWHM) of the MIL-127 NPs before and after CS coating remained unaltered, indicating a similar particle size.

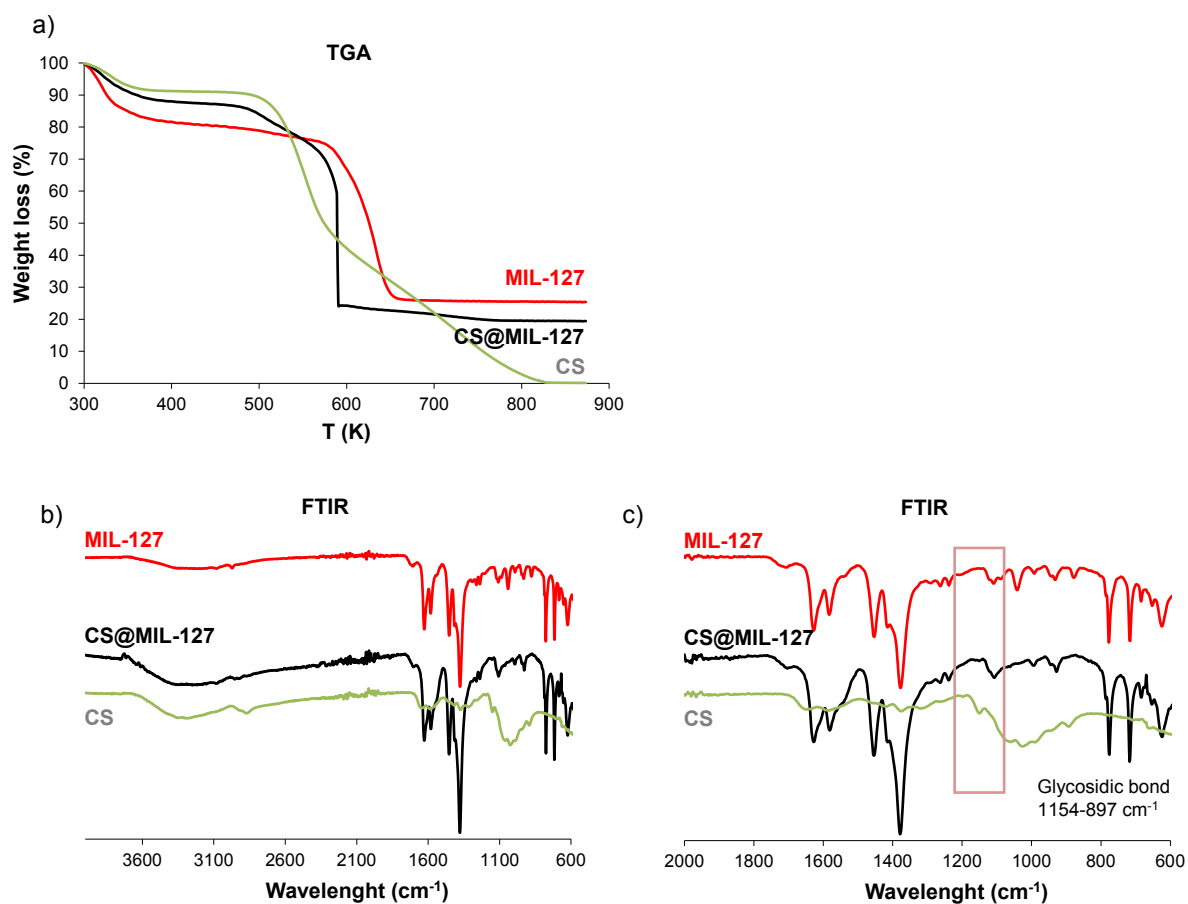


Figure S3. (a) TGA, and (b, c) FTIR of MIL-127 NPs (red), CS@MIL-127 NPs (black), and free CS (grey). Aside to the main bands attributed to MIL-127, the CS@MIL-127 NPs spectrum exhibits additional bands at 1145 cm⁻¹ assigned to the glycosidic bond, a clear indication of the presence of CS.

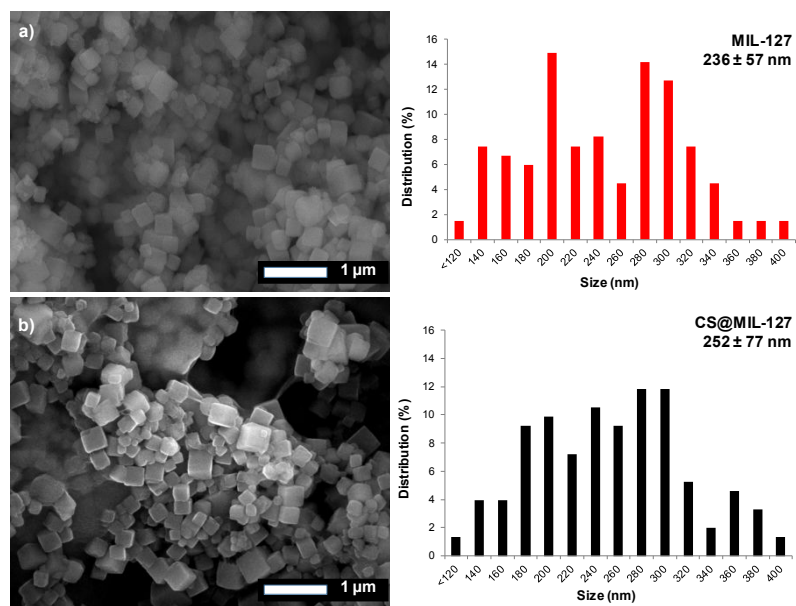


Figure S4. (a) FEG-SEM images of MIL-127 NPs (red), and (b) CS@MIL-127 NPs (black). The cubic NPs shape was maintained after CS coating. NPs size distribution was studied by SEM images using *ImageJ* software for image processing and analysis.¹ Slightly larger nanoparticles ($n \geq 150$) were obtained in CS@MIL-127, consistent with the presence of a CS layer.

S3. MOF stability under diverse physiological media

To gain a better insight into the colloidal, chemical and structural stability, MOFs were suspended in different physiological media, from simple media (pure water) to more complex ones such as simulated GI fluids like *lis*-SIF, *lis*-SIF-panc, or *lis*-SIF-muc for 24 h at 37 °C.

Colloidal stability. 1 mg of dry powder (MIL-127 or CS@MIL-127) was dispersed in 10 mL of each media (MilliQ, *lis*-SIF, *lis*-SIF-panc, or *lis*-SIF-muc). Suspensions were sonicated once (20% amplitude, 30 s) and the evolution of particle size was monitored during 24 h at 37 °C (**Figure 1**).

Chemical & structural stability. 20 mg of MIL-127 or 40 mg of CS@MIL-127 (weight considering dry powders) were suspended in 10 mL of each media (MilliQ, *lis*-SIF, *lis*-SIF-panc, or *lis*-SIF-muc). The resulting suspensions were kept in an orbital incubator shaker at 37 °C using bidimensional stirring. After different incubation times (1, 2, 5, 7 and 24 h), an aliquot of 1 mL of supernatant was recovered by centrifugation (13500 rpm, 10 min), being replaced with the same volume of fresh media at 37 °C. The ligand concentration was quantified in the solution by HPLC for determining its chemical stability profile (**Figure 1**). After the last incubation time, the MOF structural stability was study by XRPD (**Figure S5**).

MilliQ water: The uncoated MIL-127 exhibited a suitable colloidal stability up to 24 h, whereas in CS-coated MIL-127 a sedimentation phenomenon is observed between 7 and 24 h (**Figure 1**). The accumulative ligand leaching to the environment, as a consequence of a potential structure collapse, was minimum, in accordance with an excellent MOF chemical and structural stability (<2 % linker release with intact XRD patterns after 24 h in both materials).

Lis-SIF medium: Uncoated MIL-127 remains stable with a slight increase of particle size (average size $\sim 540 \pm 12$ nm) and strong negative conversion (-64 ± 1 mV) up to 24 h, while the CS coated material precipitates with time. The progressive precipitation of CS@MIL-127 NPS in this medium could be associated with a weaker electrostatic repulsion force required to stabilize the colloids (ζ -potential values -64 and 0 mV for MIL-127 and CS@MIL-127 NPs, respectively; **Table 1**). As expected, the progressive aggregation effect here observed for the uncoated particles is in agreement with the degradation data, observing that the MIL-127 framework disruption is in a greater extent than its coated homologous (25% vs. 3% of linker release, respectively), preserving both solids their crystallinity over the time (**Figure S5**).

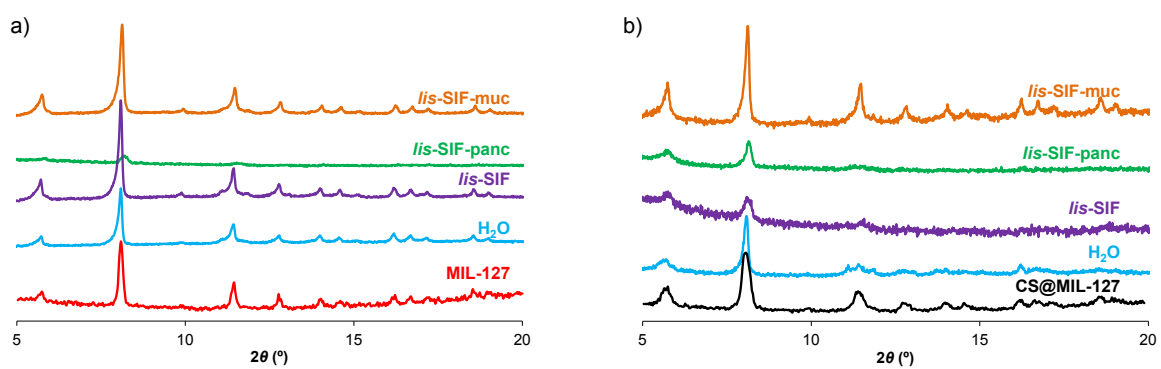


Figure S5. XRPD patterns of (a) MIL-127 and (b) CS@MIL-127 after being suspended for 24 h in water (pale blue), *lis*-SIF (purple), *lis*-SIF-panc (black), and *lis*-SIF-muc (yellow) at 37 °C.

S4. *In vitro* cell studies

Cells and culture. The murine macrophages J774.A1 cell line (ATCCTIB-67) was maintained in RPMI 1640 medium^{2,3} whereas the human color carcinoma Caco-2 cell line (ATCC HTB-37TM) was cultured in DMEM.⁴ Both media were supplemented with 1% glutamax-1, 10% of heated-inactivated FBS and 1% penicillin/streptomycin,⁵ growing at 37 °C in a humidified 5% CO₂ atmosphere. Moreover, twice a week were passaged at a density of 5×10^4 cells cm⁻² (~80% of confluence), being harvested by trypsinization (1% trypsin-EDTA solution).

Cytotoxicity assays were carried out following a previously reported procedure based on the MTT method.^{2,3} Briefly, MIL-127 & CS@MIL-127 NPs as well as their precursors (using the corresponding amount: *i*) 35.49% of CS; *ii*) 14.04 and 18.95% of FeCl₃·6H₂O; and *iii*) 26.64 and 35.97% of H₄TazBz for CS@MIL-127 and MIL-127 NPs, respectively) were incubated in a 96-well plate with adherent J774.A1 and Caco-2 cells, which were seeded 24 h prior to the assay at a density of 1×10^4 cells *per* well in supplemented RPMI and DMEM, respectively. MOF suspensions were performed in a range dilution series with cell culture media (30 μL of the sample in aqueous solution were added to a final volume of 300 μL *per* well), yielding different concentrations (from 1000 to 125 μg·mL⁻¹). Subsequently, all these treatments were added into the cells for 24 h, keeping them at 37 °C with 5% CO₂ atmosphere. The cytotoxicity was determined by adding the MTT reactant (0.5 mg·mL⁻¹ in PBS, incubated at 37 °C for 2 h) followed by a PBS washing, ending with DMSO (100 μL/well/step). Absorbance was determined at $\lambda = 539$ nm under stirring. The percentage of cell viability was calculated by the absorbance measurements of control growth and test growth in the presence of the formulations at various concentration level.

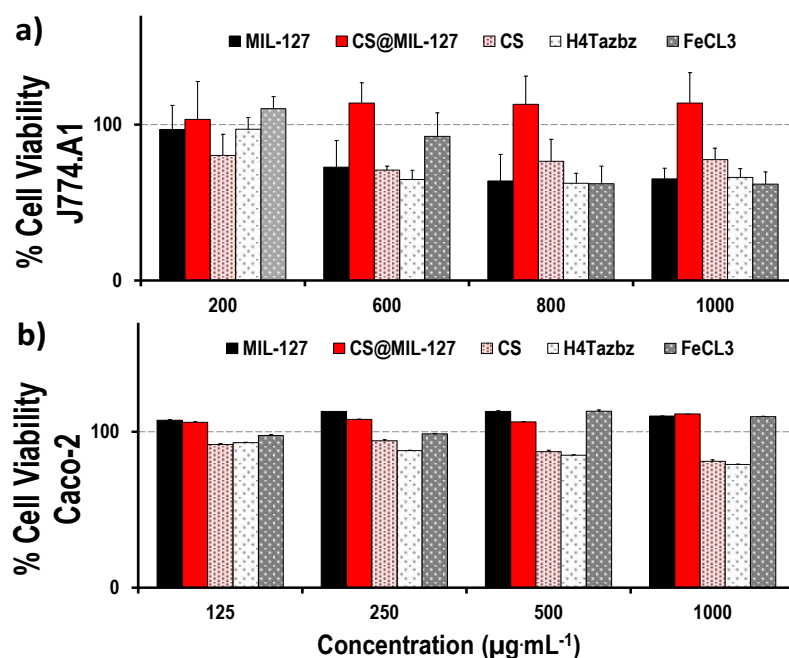


Figure S6. Cell viability of (a) J774.A1, and (b) Caco-2 cell lines after 24 h incubation with CS@MIL-127, MIL-127 NPs and precursors (CS, H₄TazBz, FeCl₃). *Note that the shown data correspond for each concentration to the average of triplicates obtained in two independent experiments ($n = 6$). The vertical error bars drawn in the diagram indicate the range of fluctuations from which the standard deviations were calculated. *NanoMOFs stability in DMEM.* The colloidal, chemical and structural stability of MOF NPs in DMEM was assessed following the same procedure as previously described for other media.

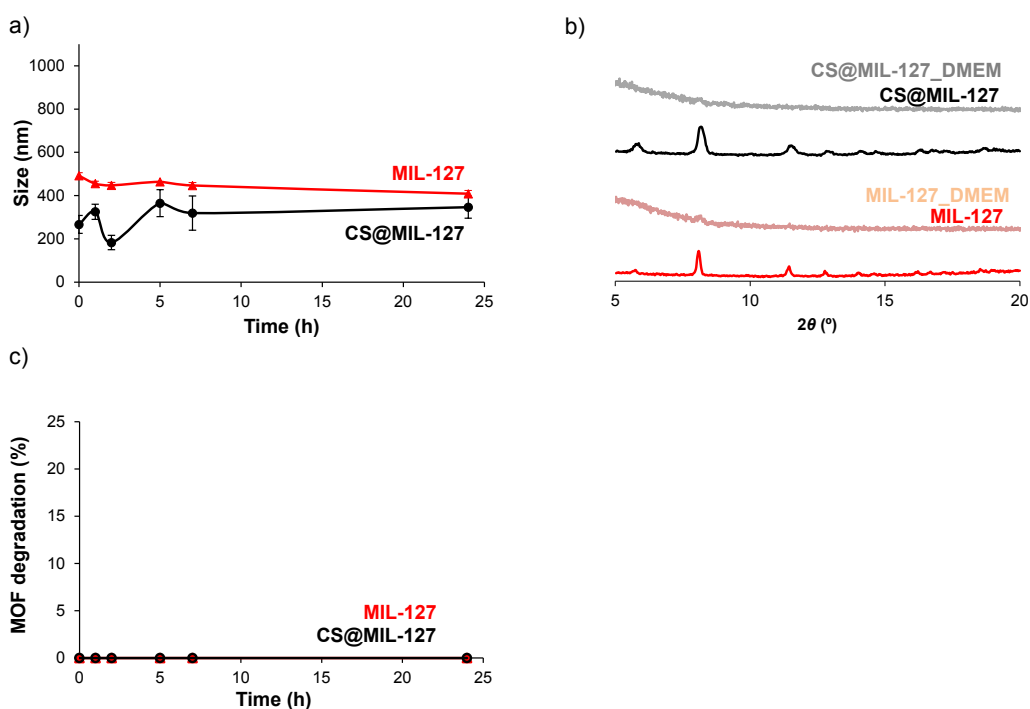


Figure S7. (a) Colloidal, (b) structural, and (c) chemical stability of MIL-127 (red) and CS@MIL-127 (black) in Dulbecco's Modified Eagle's medium (DMEM) media at 37 °C, representing the NPs size evolution (nm) or MOF degradation (%) vs. time (h).

S5. *In vivo* studies: *C. elegans*

Growth and treatment of C. elegans: N2 Bristol *C. elegans* strain and *Escherichia coli* OP50 were obtained from Caenorhabditis Genetics Center (CGC). *C. elegans* were grown on nematode growth medium (NGM) agar seeded with *E. coli* OP50 following standard practices.⁶ Synchronized worms at L4 were exposed to MIL-127 or CS@MIL-127 at (0, 500 and 1000 µg/mL) in *lis*-SIF for 24 h at 20 °C in a 24-well-plate. Survival of the worms were computed by touching the worm with an eyelash and confirming the movement. Length assay were performed to assay development, images were taken and length were computed by ImageJ after 24h. Measures were performed by triplicate (N= 3) and in total n=300 worms were analysed.

After the exposure, we performed Prussian Blue staining, a freshly mixed Perl's solution (4% KFeCN/4% HCl) was incubated with PFA fixed worms in dark for 1 h. Then, worms were cleaned with MilliQ water, centrifuged and mounted on a glass slide for observation under the stereoscope.

- M9 NaCl (5 g, 0.085 mol), KH₂PO₄ (3 g, 0.02 mol), Na₂HPO₄ (6 g, 0.04 mol), and MgSO₄ (1 mL, 1 mol/L) were dissolved in 1 L of Milli-Q water.

MOFs uptake: To quantify the amount of uptaken MOF by the worms, we separately collected the supernatant, the not ingested MOF (MOFs exposed remaining from the exposure solution), and the worms by filtration and washed with *lis*-SIF. All samples were dried at 60 °C overnight.

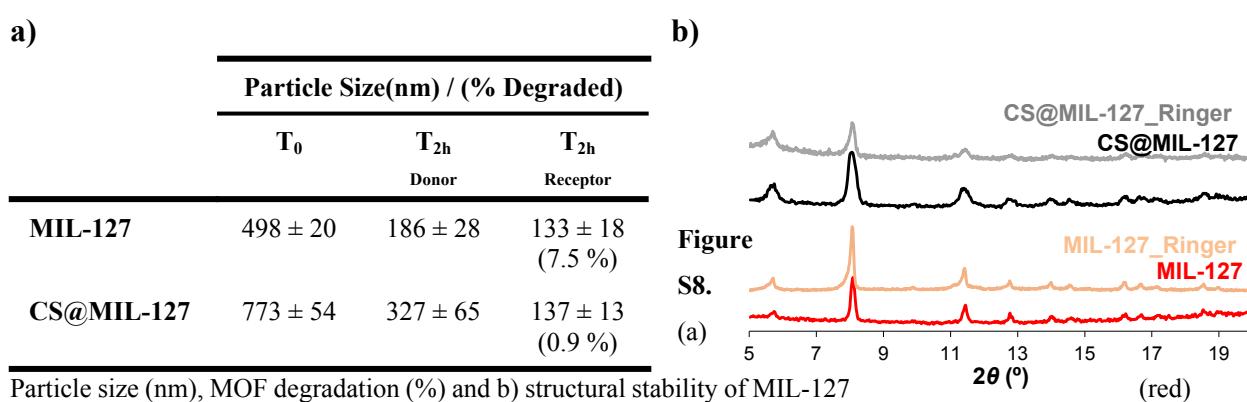
MOFs excretion assay: To assess the MOF uptake, we conducted a MOF excretion assay: filtered worms from control and treatment groups were incubated with 250 µL of *E. coli* (OD₆₀₀=0.5) with a final volume of 1 mL of *lis*-SIF for 6 h. With the presence of food, uptaken MOF could be excreted by worms.⁷ A final quantity of 1600 nematodes (n) were used *per* assay, performing three replicates (N). Then by filtration we obtained worms which excreted the MOFs and the supernatant.

The undertaken and excreted amount of MOF was determined by the amount of the linker H₄TazBz. Samples were prepared as follows: worms, supernatants (5 mL) and residual amount of MOF (not ingested) were first dried at 60 °C overnight separately. Then, 1 mL of PBS (0.5 M, pH = 2.5) was added to each sample, and the solutions were stirred for 24 h. The supernatant was collected by centrifugation and dried at 60 °C overnight. The solid residue was suspended in 4 mL of methanol (solvent in which the linker is highly soluble) during 1 h, and the supernatant was collected by centrifugation (14500 rpm, 10 min) and filtered through 0.2 µm

syringe filter. Prior to injection into the HPLC system, samples were ½-diluted in the mobile phase. The H₄TazBz quantification was performed by HPLC (see **Section S1**). The normality of data distribution was tested by one-way ANOVA test.

S6. *Ex vivo* studies: Intestinal permeability

First, the colloidal, chemical, and structural stability of MIL-127 and CS@MIL-127 under Ringer medium was assessed following the same procedure as previously described for other media. The CS@MIL-127 material shows an improved colloidal (particle size of 240 ± 124 vs. 874 ± 38 nm after 2 h) and chemical stability (~ 8 vs. 1% of MOF degradation) than the uncoated MIL-127.



For the purpose of determining the intestinal absorption of the nanoMOF formulations, *ex vivo* permeability studies were performed with fresh rat jejunum mucosal tissue by utilizing the Ussing chamber system.⁸ Female Wistar rats were fasted overnight and after sacrifice, the jejunum was removed, washing with a 0.9% NaCl solution and mounting them in the permeation chamber. During all the experiment, both compartments were oxygenated and circulated by bubbling with carbogen (95% O₂/5% CO₂), keeping the temperature at 37 °C. The bubbling of the solution is an essential factor for the viability of the intestinal membranes, but also to avoid the NPs sedimentation. The tissue biopsies were placed into the diffusion chambers and let to stabilize during 0.5 h. The tissue viability and integrity were controlled by monitoring the transepithelial resistance (TEER) using a Millicell®ERS-2 meter.⁹ Biopsies were placed with the gut inner area (*intestinal mucosa*, representing the *lumen*) faced to the donor compartment with the outermost gut *serosa* layer (representing the *blood circulation*) to the receptor, leaving an available diffusion area of 1 cm². MIL-127 & CS@MIL-127 NPs (both at 2 mg·mL⁻¹) were resuspended in a bubbled Ringer solution at the donor compartment, being compared with diverse controls: *i*) a blank control only with Ringer media, and *ii*) H₄TazBz

ligand with the corresponding amount of $0.6 \text{ mg} \cdot \text{mL}^{-1}$. Permeation studies were performed for 2 h at $37 \text{ }^\circ\text{C}$. The intestinal permeation was monitored by collecting several aliquots (1 mL) from the receptor compartment at different time points (0.5, 1, 1.5 and 2 h) and replaced with the equal volume of fresh pre-equilibrated medium at the experimental temperature conditions ($37 \text{ }^\circ\text{C}$). At the end of each experiment, the collected aliquots were analyzed by: *i*) *DLS*, for particle size determination (**Figure S9**); *ii*) *ICP-OES*, for assessing the intestinal MOF NPs crossing by following the iron permeation into the receptor chamber. Note that the Fe concentration could arise from the potential disruption of the framework (NPs degradation) or from the post-treatment performed to each sample (24 h incubating the nanoMOF pellet in a high buffered solution: PBS (0.5 M), pH = 2.5) with the main purpose of quantifying the total bypassed amount; *iii*) *TEM*, observing the MOF NPs; and *iv*) *histological examination*, assessing the presence of MOF NPs within the tissue. In particular, for this histological observation the jejunum was excised and fixed overnight in 4% *p*-formaldehyde. Once washed with PBS (pH= 7.4), they were stored in EtOH solution (70%) and stained with Perl Prussian blue dye for the observation of the Fe-MOF NPs, and hematoxylin and eosin routinely for histological examination.

Moreover, the intestinal diffusion flux ($\mu\text{g} \cdot \text{cm}^{-2} \cdot \text{mL}^{-1} \cdot \text{h}^{-1}$) was calculated by using the equation $F = (dQ/dt)/A$, where dQ/dt ($\mu\text{g} \cdot \text{mL}^{-1} \cdot \text{h}^{-1}$) represents the permeability rate, and A (cm^2) is the effective surface area of the intestinal mucosa. Moreover, the permeability coefficient (P , $\text{cm} \cdot \text{h}^{-1}$) was calculated by using the equation $P = F/Q$, where Q ($\mu\text{g} \cdot \text{mL}^{-1}$) is the initial concentration of the studied compound in the donor chamber. All samples were evaluated in 6 independent experiments ($n = 6$).

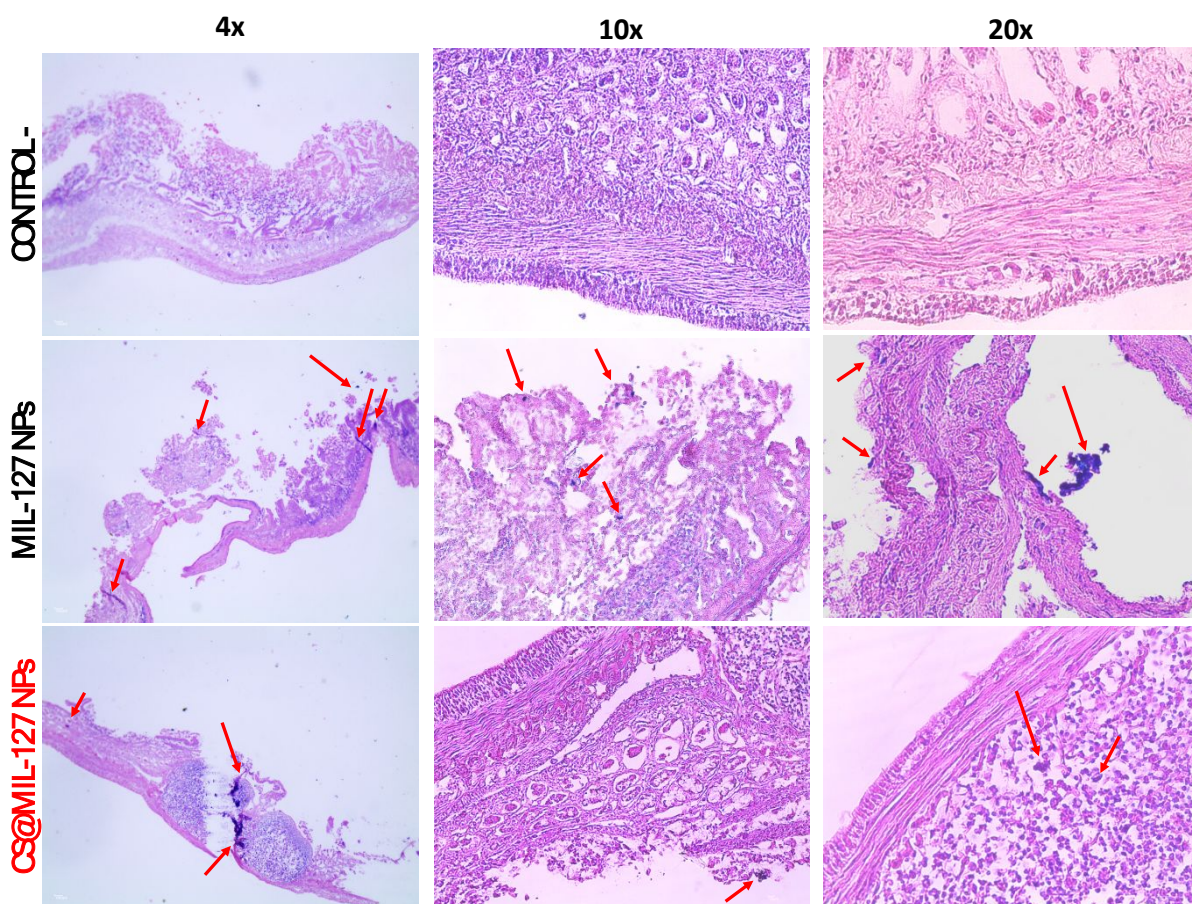


Figure S9. Histological sections of rat jejunum mucosa after 2 h of in contact with: Ringer solution (negative control), CS@MIL-127 NPs and MIL-127 NPs (red arrows).

Table S1. TEER measurement provided by the conductivity of rat intestinal cells after 2 h in contact with CS@MIL-127 and MIL-127 NPs together with their controls (untreated membrane and H₄Tazbz).

	TEER (OMH/Cm ²)			
	Untreat	H ₄ Tazbz	MIL-127	CS@MIL-127
	d Cells			
T ₀	145.54	164.52	135.70	149.02
T _{2h}	166.20	179.61	187.82	189.35

S7. Statistics

The results of the different assays are represented as mean \pm standard deviation (SD). Ordinary Two-way ANOVA analysis of variance followed by a Tukey's multiple comparison tests were carried out to determine significant differences using GraphPad Prism 7 software (GraphPad Software, Inc., La Jolla, CA, USA). Each experiment was performed at least three times ($n \geq 3$). In the graphs, the results are indicated as: $P > 0.05$, $*P \leq 0.05$, $**P \leq 0.01$, $***P \leq 0.001$ and $****P \leq 0.0001$.

S8. References

- (1) Abramoff, M. D.; Magalhaes, P. J.; Ram, S. J. Image Processing with ImageJ. *Biophotonics Int.* **2004**, *11*, 36–43.
- (2) Bellido, E.; Hidalgo, T.; Lozano, M. V.; Guillevic, M.; Simón-Vázquez, R.; Santander-Ortega, M. J.; González-Fernández, Á.; Serre, C.; Alonso, M. J.; Horcajada, P. Heparin-Engineered Mesoporous Iron Metal-Organic Framework Nanoparticles: Toward Stealth Drug Nanocarriers. *Adv. Healthc. Mater.* **2015**, *4*, 1246–1257. <https://doi.org/10.1002/adhm.201400755>.
- (3) Kong, B.; Seog, J. H.; Graham, L. M.; Lee, S. B. Experimental Considerations on the Cytotoxicity of Nanoparticles. *Nanomedicine* **2011**, *6* (5), 929–941.
- (4) Hidalgo, T.; Giménez-Marqués, M.; Bellido, E.; Avila, J.; Asensio, M. C.; Salles, F.; Lozano, M. V.; Guillevic, M.; Simón-Vázquez, R.; González-Fernández, A.; Serre, C.; Alonso, M. J.; Horcajada, P. Chitosan-Coated Mesoporous MIL-100(Fe) Nanoparticles as Improved Bio-Compatible Oral Nanocarriers. *Sci. Rep.* **2017**, *7*, 43099–43113. <https://doi.org/10.1038/srep43099>.
- (5) Tamames-Tabar, C.; Cunha, D.; Imbuluzqueta, E.; Ragon, F.; Serre, C.; Blanco-Prieto, M. J.; Horcajada, P. Cytotoxicity of Nanoscaled Metal–Organic Frameworks. *J. Mater. Chem. B* **2014**, *2*, 262–271. <https://doi.org/10.1039/c3tb20832j>.
- (6) Brenner, S. The Genetics of *Caenorhabditis Elegans*. *Genetics* **1974**, *77* (1), 71–94.
- (7) Gonzalez-moragas, L.; Yu, S. M.; Carenza, E.; Laromaine, A.; Roig, A. Protective Effects of Bovine Serum Albumin on Superparamagnetic Iron Oxide Nanoparticles Evaluated in the Nematode *Caenorhabditis Elegans*. *ACS Biomater. Sci. Eng.* **2015**, *1* (11), 1129–1138. <https://doi.org/10.1021/acsbiomaterials.5b00253>.
- (8) Woitiski, C. B.; Sarmiento, B.; Carvalho, R. A.; Neufeld, R. J.; Veiga, F. Facilitated Nanoscale Delivery of Insulin across Intestinal Membrane Models. *Int. J. Pharm.*

- 2011**, *412* (1–2), 123–131. <https://doi.org/10.1016/j.ijpharm.2011.04.003>.
- (9) Development, O. for E. C. and. Guidance Document for the Conduct of Skin Absorption Studies. *OECD Environmental Health and Safety Publications*. 2004, pp 1–31. <https://doi.org/10.1787/9789264078796-en>.